



Heterogeneous nucleation of polymorphs on polymer surfaces: polymer–molecule interactions using a heterogeneous dielectric solvation model

Nanna Wahlberg¹ · Anders Ø. Madsen² · Kurt V. Mikkelsen¹ 

Received: 8 December 2017 / Accepted: 13 April 2018 / Published online: 9 June 2018
© Springer-Verlag GmbH Germany, part of Springer Nature 2018

Abstract

We have investigated the mechanism of the nucleation of acetaminophen on poly(methyl-methacrylate) and poly(vinyl-acetate) utilizing a combination of quantum mechanical computations and electrostatic models. We have used a heterogeneous dielectric solvation model to determine the stability of different orientations of acetaminophen on polymer surfaces. We find that for the nucleation of acetaminophen on the polymer surfaces in vacuum, the most stable orientation is a flat orientation. For the nucleation process in solution where acetaminophen and the polymer surface are surrounded by a solvent, we find that the heterogeneous dielectric solvation model predicts that a sideways orientation is the most stable orientation.

Keywords Acetaminophen · Poly(methyl methacrylate) · Poly(vinyl acetate) · Heterogeneous dielectric solvation model · Interfaces

Introduction

Polymorphism is the ability of atoms or molecules to assemble in several different crystalline structures. It is a common phenomenon that has been used to elucidate structure–property relationships in solid-state organic chemistry for decades [1, 2]. Most molecular systems may exhibit polymorphism—and it has been postulated that it is a matter of the amount of resources used to investigate the system that determines the number of polymorphs discovered [3].

Generally, we consider the ability to predict and control the structure of crystals of paramount importance in the production of new solid-state materials. An example is the production of active pharmaceutical ingredients for solid-state dosage forms, where it is vital to produce crystal forms

with dissolution and solubility properties that ensure sufficient bioavailability of the compound. It is also important to obtain a solid form that is easy to manufacture and that is stable during transportation and storage. These properties all depend on the crystal structure. The sudden appearance of new crystal forms may be disastrous for the production of pharmaceuticals, as was the case for the HIV drug ritonavir [4]. Last, there are legal issues related to the patentability of new crystal forms [5].

The strategy of most pharmaceutical companies is to screen for polymorphism using a range of crystallization strategies. The strategies involve screening different solvents, temperatures, pH values, etc. The outcome is typically evaluated using powder X-ray crystallography. These experimental screening techniques are tedious and costly, and there is no guarantee that all possible polymorphs have been determined. There is evidently a demand for complementary computational tools that can predict the most likely structures and suggest a strategy to obtain them.

A computational strategy to predict crystal structures has been pursued for decades. Within the last years, several successful approaches have been presented as part of the crystal structure prediction blind tests [6]. These approaches all search for the global minimum on the potential energy hypersurface of crystal coordinates. In spite of several successful

This paper belongs to Topical Collection XIX - Brazilian Symposium of Theoretical Chemistry (SBQT2017)

✉ Kurt V. Mikkelsen
kmi@chem.ku.dk

¹ Department of Chemistry, University of Copenhagen, Universitetsparken 5, 2100 Copenhagen Ø, Denmark

² Department of Pharmacy, University of Copenhagen, Universitetsparken 2, 2100 Copenhagen Ø, Denmark

predictions of crystal structures, it remains difficult to assess the relative energies of polymorphic systems [7]. A plausible explanation for these problems is that the potential energy differences between polymorphic forms are so small (1–2 kJ/mol) that the determining factors for polymorph selection must be explained in terms of differences in free energy, including the vibrational entropy [8–11]. Another explanation is that the structures used are not sufficiently accurate [12]. Kinetic factors may also play an important role, so that the observed structure may be determined by the nucleation and growth of crystals, rather than to the thermodynamic stability of the final crystalline state [1, 2]. In this contribution, we investigate the role of nucleation.

In the early stages of crystal formation, the formation of pre-nuclear clusters, the nucleation stage, and the subsequent growth of crystals, solvent effects, and temperature can influence the growth rates of specific crystal surfaces [13–16], and heterogeneous nucleation events involving the crystallization vessel or other surfaces can mediate a preference for nucleation of a specific crystal form. Selection of crystal forms, and modification of crystal habits have been demonstrated by epitaxial growth on Langmuir–Blodgett films by Leiserowitz and coworkers [13]. As demonstrated by Matzger and coworkers [17], it is also possible to influence the polymorph selection by using polymer heteronuclei. Polymer-induced heteronucleation (PIHn) has been proposed and tested as a method for discovering new solid forms. The method has been demonstrated for small molecules [17], supramolecular complexes [18], and proteins [19]. In spite of the success of these investigations for scanning for polymorphism, and for promoting new polymorphic forms, little is understood about the underlying mechanism,

hampering progress in the design of experimental protocols that can be used to explore the landscape of polymorphic crystal forms.

Because of the largely amorphous character of the solid polymers, epitaxial growth is not a likely explanation for the polymer's ability to induce different polymorphs. In the work presented here, we investigate whether a heterogeneous solvation model based on electrostatic interactions between the surface and the crystal nuclei can provide new insights into the mechanism of polymorph selection by heterogeneous nucleation. The model system used is acetaminophen (ACM, Fig. 1), a common drug, which crystallizes in a monoclinic and an orthorhombic form. The monoclinic form is known to be the thermodynamically stable form at ambient conditions [20]. Acetaminophen is a commonly used model system in the study of polymorphic molecular crystals. The polymer-induced nucleation of the two forms has previously been studied [17]. Most recently, López-Mejías and coworkers have investigated the heteronucleation by a combined experimental and computational approach, where polymer-covered surfaces were used to facilitate nucleation. The preferred orientation of acetaminophen crystals on these surfaces were determined using powder X-ray crystallography, and the results were compared to force-field based docking calculations of polymers on crystal surfaces [21].

We wish to investigate how acetaminophen interacts with a polymer particle in order to understand how the polymer particle facilitates nucleation. Our aim is to study this for the molecule–polymer particle system in vacuum and in solution. Furthermore, we consider different conformations and orientations of acetaminophen approaching a polymer

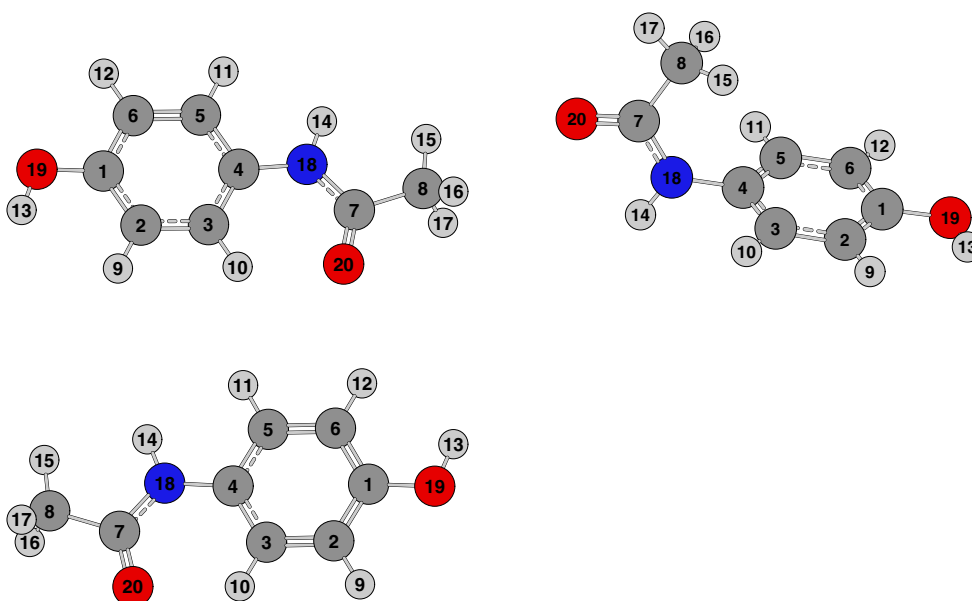


Fig. 1 The conformations of acetaminophen with labeled atoms

particle in order to investigate preferential nucleation to the polymer particle.

Our model is based on the use of energy functionals for dielectric media and generally the basic idea is to divide a large system into two or more subsystems depending on the actual system. The subsystem of principal interest, acetaminophen, will be described by a quantum mechanical approach, whereas the other subsystems are described by classical electrostatics [22–62]. We determine the interactions between the molecular subsystem and the polymer particle by the induced polarization in the polymer particle and the electric field due to the charge distribution of the molecular subsystem [22–62]. The molecular subsystem and classical subsystems are coupled by an effective interaction operator and thereby one obtains a modified quantum mechanical equation for calculating the interaction energy of a molecular subsystem interacting with the polymer particle in vacuum or in solution. We consider the molecular subsystem, acetaminophen, to interact with the polymer particle and the surrounding solvent and we utilize a heterogeneous solvation model [63–65] for calculating the interaction energies of the different conformations and orientations of acetaminophen with the heterogeneous environment.

Theory

The heterogeneous solvation model for the polymer and molecular system in vacuum

Heterogeneous and homogeneous solvent effects and the interactions between particles and molecules have been treated in a number of models and the general trend in these models is to divide the system into a molecular and a surrounding part, and treat the two subsystems with different levels of theory. This could be quantum mechanics/molecular mechanics models or a heterogeneous solvation model where the molecule interacts with a particle represented by a dielectric medium. The later model is the approach taken in the following.

We consider the heterogeneous solvation model containing a molecule and a polymer particle subsystem and the outer solvent is neglected. The polymer particle is represented by a semi-infinite dielectric medium, and the coordinate system is defined so $z = 0$ is the interface between the two subsystem. Further, the coordinate system is restrained by the dielectric medium being located at $z < 0$ and the molecule at $z > 0$. The molecule is represented by quantum mechanically determined partial charges located at the atomic positions. The molecular partial charges are determined prior to this, by either the scheme proposed by Cioslowski [67–69] or the CHelpG [70] method. Since the

interface is at $z=0$ the z component of the point charge q_i at the position $\vec{r}_i = (x_i, y_i, z_i)$ is restricted to $z_i > 0$.

The interaction between the charges and the dielectric medium is modeled by image charges in the dielectric medium. The image charges and their positions are given by

$$q_{i,s} = -\frac{\epsilon - 1}{\epsilon + 1}q_i \quad (1)$$

at $\vec{r}_{i,s} = (x_i, y_i, -z_i)$

where the subscript s refers to an image charge.

The induced potential from N image charges at an arbitrary point in the molecular subsystem, \vec{r} is given by

$$U_{pol}(\vec{r}) = \sum_{i=1}^N U_{pol}^{(i)}(\vec{r}) = \sum_{i=1}^N \frac{q_{i,s}}{|\vec{r} - \vec{r}_{i,s}|} \quad (2)$$

The energy resulting from the interaction between the molecular charge distribution, ρ_m , and the dielectric medium is given by

$$E_{pol} = \frac{1}{2} \int d\vec{r} \rho_m(\vec{r}) U_{pol}(\vec{r}) \quad (3)$$

Since the distribution of the molecular charges is discrete, the integral can be substituted with a summation:

$$E_{pol} = \frac{1}{2} \sum_{k=1}^N q_k U_{pol}(\vec{r}_k) \quad (4)$$

It is important to note that the potential in Eq. 2 is the potential arising from the interaction between one point in the molecular subsystem with all the image charges in the dielectric medium, i.e., a sum over all the image charges. On the other hand, (4) is a sum over all the charges and potentials in the molecular subsystem.

The heterogeneous solvation model for the polymer and molecular system in solution

The dielectric continuum model above neglects that the molecule in many cases is surrounded by a medium other than vacuum. The inclusion of a surrounding solvent in the heterogeneous solvation model is done by including in addition to the dielectric continuum at $z < 0$ a second dielectric medium placed at $z > 0$ and $\sqrt{x^2 + y^2 + z^2} > a$ with a being the radius of a half-sphere cavity containing the molecule. The first medium is the solid particle and modeled by the dielectric constant ϵ_1 , while the second dielectric medium is the solvent with the dielectric constant ϵ_2 . In this model, each charge in the molecular system gives rise to three new image charges; an image charge directly induced in the solid continuum q_{s1} , an image charge in the solvent continuum q_{s2} , and an image charge induced in the solid q_{s3}

Fig. 2 Slabs of the monoclinic and orthorhombic forms of acetaminophen with the most energetically favorable orientation towards the polymer surface

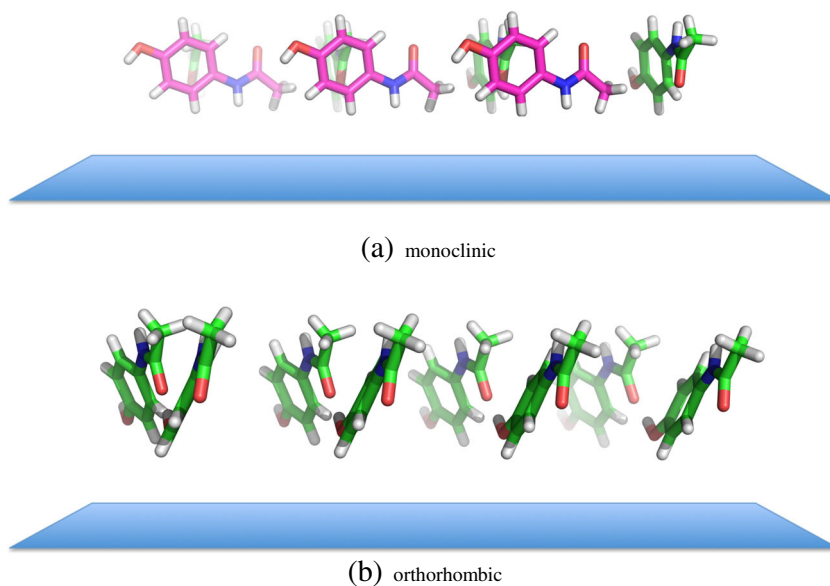


Table 1 The partial charges of acetaminophen in the flat and scorpion conformations, derived using the CHelpG method and CAM-B3LYP and different basis sets

| | Af cc-pVQZ | aug-cc-pVQZ | As cc-pVQZ | aug-cc-pVQZ | Ac cc-pVQZ | aug-cc-pVQZ |
|------------|---------------|-------------|---------------|-------------|---------------|-------------|
| C(1) | 0.3785 | 0.3873 | 0.3840 | 0.3904 | 0.3714 | 0.3802 |
| C(2) | -0.2874 | -0.2866 | -0.1528 | -0.2983 | -0.1761 | -0.1737 |
| C(3) | -0.1993 | -0.2029 | 0.0030 | -0.1394 | -0.2517 | -0.2568 |
| C(4) | 0.4103 | 0.4228 | 0.3216 | 0.3213 | 0.4078 | 0.42078 |
| C(5) | -0.296 | -0.3010 | -0.1983 | -0.1968 | -0.2357 | -0.2392 |
| C(6) | -0.1515 | -0.1499 | -0.1857 | -0.1842 | -0.2653 | -0.2652 |
| C(7) | 0.8200 | 0.8335 | 0.7684 | 0.7813 | 0.8502 | 0.8649 |
| C(8) | -0.4392 | -0.4437 | -0.2563 | -0.2566 | -0.4826 | -0.4892 |
| H(9) | 0.1304 | 0.1299 | 0.1390 | 0.1389 | 0.1416 | 0.1403 |
| H(10) | 0.1901 | 0.1912 | 0.1249 | 0.1228 | 0.1887 | 0.1906 |
| H(11) | 0.1378 | 0.1381 | 0.1251 | 0.1225 | 0.1376 | 0.1376 |
| H(12) | 0.1402 | 0.1398 | 0.1476 | 0.1473 | 0.1307 | 0.1309 |
| H(13) | 0.4070 | 0.4042 | 0.4038 | 0.4016 | 0.3945 | 0.3918 |
| H(14) | 0.3337 | 0.3327 | 0.3168 | 0.3143 | 0.3156 | 0.3148 |
| H(15) | 0.0984 | 0.1002 | 0.0495 | 0.0490 | 0.1167 | 0.1189 |
| H(16) | 0.1244 | 0.1247 | 0.0796 | 0.0795 | 0.1315 | 0.1319 |
| H(17) | 0.1245 | 0.1247 | 0.0826 | 0.0827 | 0.1316 | 0.1321 |
| N(18) | -0.701 | -0.7112 | -0.6547 | -0.6538 | -0.7017 | -0.7126 |
| O(19) | -0.6009 | -0.6066 | -0.5811 | -0.5856 | -0.5841 | -0.5899 |
| O(20) | -0.6194 | -0.6273 | -0.6293 | -0.6395 | -0.6197 | -0.6282 |
| RMS | 0.0033 | 0.0034 | 0.0031 | 0.0032 | 0.0034 | 0.0035 |
| Dipole | 2.284 | 2.317 | 4.460 | 4.471 | 4.804 | 4.820 |
| Energy*/eV | - | - | 0.1095 | 0.1100 | 0.0172 | 0.0171 |

Results are in atomic units

*The energies are given relative to the energy obtained for the **af** conformation

by the induced charge in the solvent q_{s2} . Thus, the charge q_i at $r_i = (x_i, y_i, z_i)$ in the molecular system induces the following image charges

$$q_{i,s1} = -\frac{\epsilon_1 - 1}{\epsilon_2 + 1} q_i \text{ at } \vec{r}_{i,s1} = (x_i, y_i, -z_i) \quad (5)$$

$$q_{i,s2} = -\frac{a}{|\vec{r}_i|} \frac{\epsilon_2 - 1}{\epsilon_2 + 1} q_i \text{ at } \vec{r}_{i,s2} = \frac{a^2}{|\vec{r}_i|^2} (x_i, y_i, z_i) \quad (6)$$

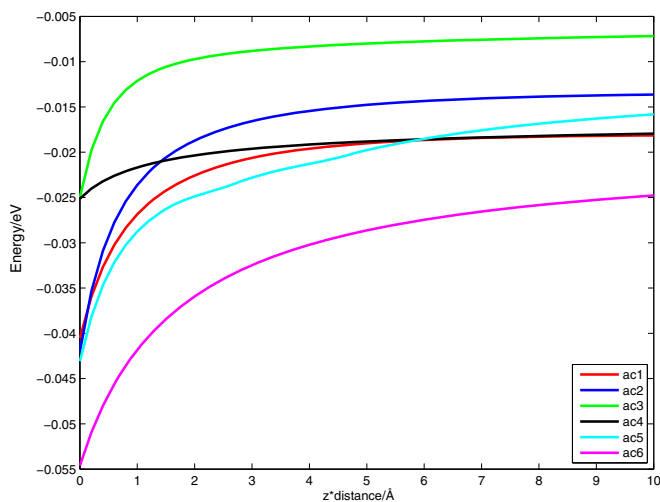
$$q_{i,s3} = -\frac{\epsilon_1 - 1}{\epsilon_2 + 1} q_{i,s2} \text{ at } \vec{r}_{i,s3} = \frac{a^2}{|\vec{r}_i|^2} (x_i, y_i, -z_i) \quad (7)$$

The induced potential from the 3N charges at an arbitrary point \vec{r} in the half-sphere cavity is given by

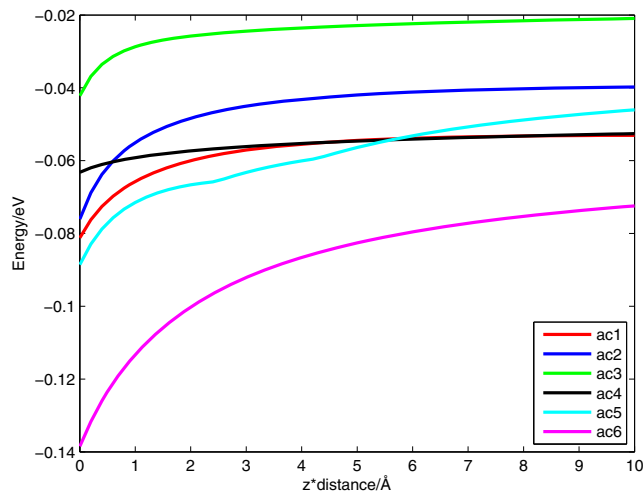
$$U_{pol,solv}(\vec{r}) = \sum_{i=1}^N U_{pol}^{(i)}(\vec{r}) = \sum_{i=1}^N \sum_{j=1}^3 \frac{q_{i,sj}}{|\vec{r} - \vec{r}_{i,sj}|} \quad (8)$$

and we find that the energy of the interaction between molecule and solvent, and solid particle is obtained as

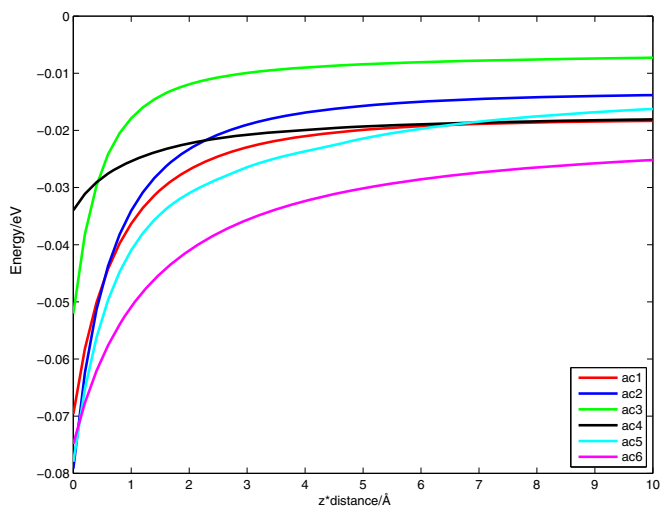
$$E_{pol,solv} = \frac{1}{2} \int d\vec{r} \rho_m(\vec{r}) U_{pol,solv}(\vec{r}) \quad (9)$$



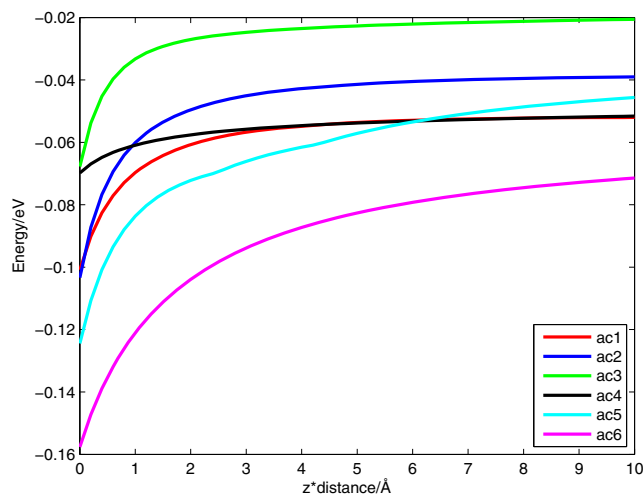
(a) Surface $\epsilon = 2$, Solvent $\epsilon = 2$.



(b) Surface $\epsilon = 2$, Solvent $\epsilon = 100$.



(c) Surface $\epsilon = 20$, Solvent $\epsilon = 2$.



(d) Surface $\epsilon = 20$, Solvent $\epsilon = 50$.

Fig. 3 Energies of the **af** conformation as a function of the distance to the surface, using different combinations of dielectric constants for the solvent and surface

and since the molecule is represented by a set of discrete quantum mechanically determined charges, the integral is substituted by a summation

$$E_{pol,solv} = \frac{1}{2} \sum_{k=1}^N q_k U_{pol,solv}(\vec{r}_k) \quad (10)$$

and the radius of the half spherical cavity is determined by the atom where the distance to origin plus the van der Waal radius of that given atom is largest (Fig. 2).

Results and discussion

In this study, we consider three conformations of acetaminophen, Fig. 1, approaching a polymer surface. In addition, each conformer is approaching the surface in six different orientations (Figs. 6 and 11).

The molecular structures were determined by geometry optimization at the CAM-B3LYP/aug-cc-pVTZ level of theory. The partial molecular charges were calculated from the geometries using the CHelpG procedure implemented in the Gaussian electronic structure program [66] with different basis set (see Table 1). The partial charges were converged when using the aug-cc-pVQZ basis set, and the partial charges were used in the heterogeneous solvation model for calculating the interaction energy. The polymer particle was represented as a dielectric medium with a dielectric constant, ϵ_1 , set to 10 and the solvent used here is water and represented as a dielectric medium with the dielectric constant $\epsilon_2 = 78$

In Figs. 4, 7, and 9, the interaction energies between the polymer particle and acetaminophen in the flat and scorpion conformations are plotted for all orientations. It must be

emphasized that the distance axis is not equivalent to the z component of the position vector. The distance axis is zero when the van der Waal radius of the molecule equals the distance from the closest atom to the surface. It should be mentioned that the van der Waal radius is not the same in all directions, that is, the closest atom at different orientations is not necessarily at the same distance from the surface. To avoid mixing, the z component of the position and the distance from the van der Waal radius, the later is renamed z^* . The van der Waal radii used for the respective atoms are, $r_w(C) = 1.70\text{\AA}$, $r_w(H) = 1.20\text{\AA}$, $r_w(O) = 1.50\text{\AA}$, and $r_w(N) = 1.55\text{\AA}$.

The interaction energies of the solvated molecule are shown as a function of the distance z^* (Fig. 3).

The polymer and molecular system in vacuum

The flat conformation, af In Figs. 4 and 5, the interaction energies between the polymer and acetaminophen in the flat conformation are plotted for all six orientations in standard and logarithmic scale. The **af5** orientation has the lowest energy closely followed by the **af2** orientation. This is due to the large negative charge on the nitrogen and oxygen atoms in the amide group, the oxygen atom in hydroxy group, and the corresponding induced positive charge in the dielectric medium. The reason for the **af5** orientation to have slightly lower energy than the **af2** orientation is that the positively charged carbon atom in the amide group is further away from the positive charge induced by the oxygen of the same group. In the **af2** orientation, all the atoms in the amide group are close to the surface and thereby the induced charges. Since the central carbon in the amide group, C(7), is positively charged, all the surrounding negatively charged atoms, N(18), O(20), and C(8), are repelled by the induced

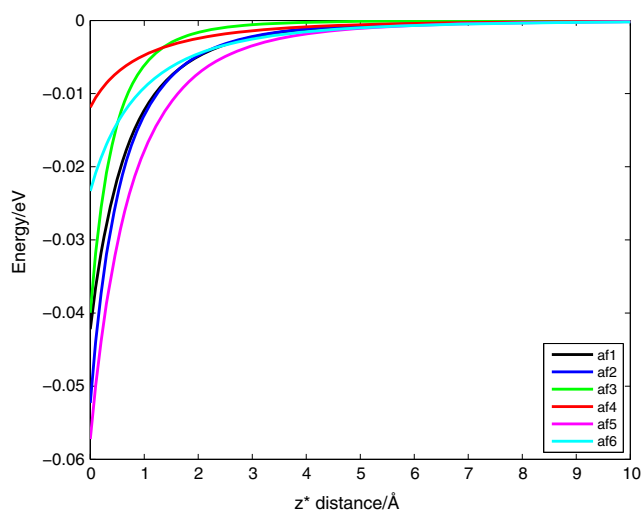


Fig. 4 Energy plots of the six orientations of the flat conformations of acetaminophen

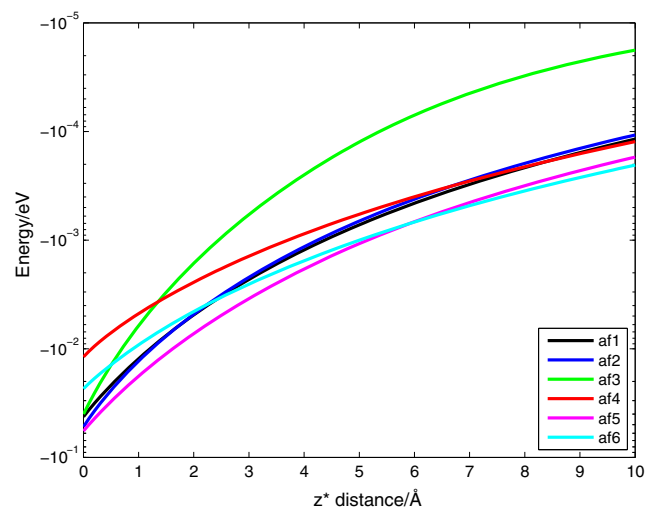


Fig. 5 Energy plot of the six orientations of the flat conformation of acetaminophen in a logarithmic scale

negative charge and vice versa. This repulsion is larger than the gain in partial charges of the atoms being close to the surface.

The **af1** orientation behaves overall very similar to that of the **af2** orientation, which is expected due to the similarity in orientation. The difference between **af1** and **af2** is the angle between the benzene moiety and the surface; in **af1** they are parallel, while the benzene moiety is tilted in **af2** so the line connecting the lower hydrogen atom in the methyl group and the hydroxy group are parallel to the surface. At long distances, the interaction energies of the two orientations are almost identical. When the molecules are within a distance of 1.5 Å, ($z^* = 1.5$), the energy of the **af2** orientation drops significantly compared to **af1**, the reason being that the hydroxy oxygen, O(19), is closer to the surface in this orientation.

The **af1** orientation has a slightly lower energy than the **af3** orientation at $z^* = 0$, but as the distance is increased, the energy difference increases as well, to around $z^* = 2$, from where it decreases again. In the logarithmic plot it is clearly observed that the **af3** orientation is significantly less stable than the rest of the orientations at distances longer than 2 Å. In the **af3** orientation, the hydroxy group is the driving force in the increased interaction energy. Since the amide group at all times is approximately 4 Å further away from the surface, the interaction energy contribution from this part of the molecule plays a less significant role. At short distances, however, the proximity of the hydroxy group and dielectric medium results in lower energies than **af6** and **af4**. The proximity of the hydroxy group has, in the **af6** orientation, been sacrificed to get the amide group closer to the surface, but since the oxygen in this group is pointing away, the resulting interacting energy at zero distance is lowered.

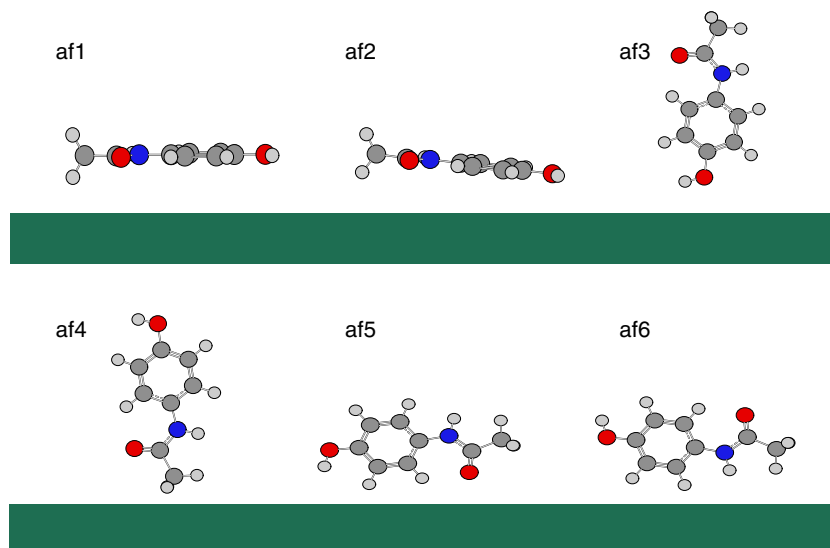
The **af6** and **af4** orientations have remarkably higher interaction energies than the rest of the orientations. This

is due to a strong induction of a negative charge, by C(7), in the proximity of the negatively charged C(8) and N(18). In all the other cases, the amide oxygen, O(20), and/or the hydroxy oxygen, O(19), have been closer to the surface, and thus contributed to a large interaction. In **af6**, these effects are strongly decreased. Though somewhat counter intuitive, the lowest interaction energy is observed in the case of orientation **af4**. One might suspect this orientation to yield a lower interaction energy due to the amide pointing down towards the dielectric medium, but this is obviously wrong. The reason for the smaller energy contribution may be found in the increased distance from the surface to the charged nitrogen and oxygen in the amide group. Furthermore, the positively charged carbon, C(7), is closest to the surface and thereby inducing a negative charge close to the negatively charged carbon in the methyl group.

The ac conformation The only difference between the two flat conformations **af** and **ac** is the direction of the hydroxy bond compared to the amide group. In **af**, the N–H bond is in the opposite direction of the O–H bond, while in **ac** the bonds are in the same direction. In Table 1 the charges of **ac** with cc-pVQZ and aug-cc-pVQZ basis sets are listed. The atomic charges of **af** and **ac** are overall the same, but the **ac** conformation has slightly larger charges and significantly larger dipole moment.

The investigated orientations of the **ac** conformation are the same as those for **af** and named in the same manner (see Fig. 6). Because of the high degree of similarity between the conformations, the orientations of **af** and **ac** are expected to behave similarly. The difference in dipole moment does, however, indicate there might be some changes. Indeed, the relative stability and the minimum energy have been changed (Fig. 7): the lowest energy is now obtained by

Fig. 6 The orientations of the flat conformations



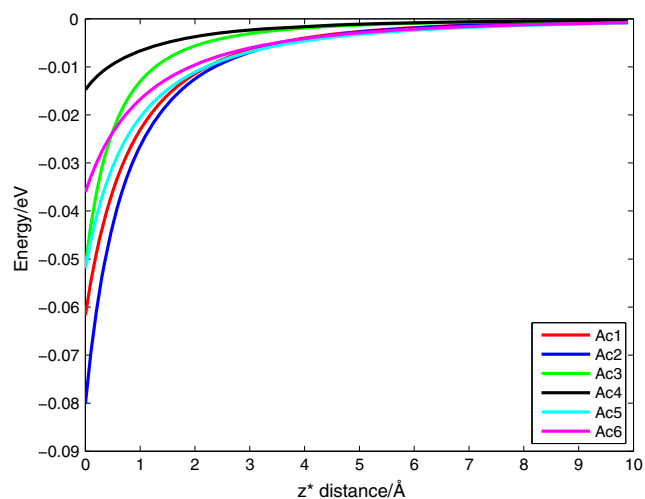


Fig. 7 Energy plots of the six orientations of the flat **ac** conformations of acetaminophen

orientation 2, which gains about -0.03 eV, while orientation 5, which has the lowest energy in **af**, is elevated by 0.01 eV.

The two orientations parallel or almost parallel to the surface, 1 and 2, are stabilized by the rotation of the O–H bond. The reason for this is that the negative induced charge from the hydroxy hydrogen is further away from O(20). This can be seen as an energy lowering of O(20) and H(13) for orientation 1 and 2 in **ac** conformation compared to **af** (Fig. 12). One might expect this to be a minor change, but the energy contribution from these atoms is decreased; the difference is about 0.065 eV, on the same scale as the overall energy (Fig. 8).

The sideways orientations, 5 and 6, are raised or lowered in energy depending on whether H(13) is pointing down towards the surface or away from it. The energy is lower

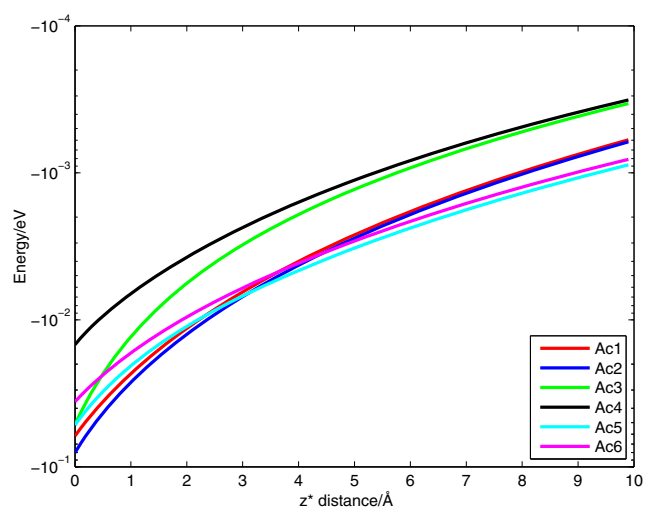


Fig. 8 Energy plot of the six orientations of the flat **ac** conformation of acetaminophen in a logarithmic scale

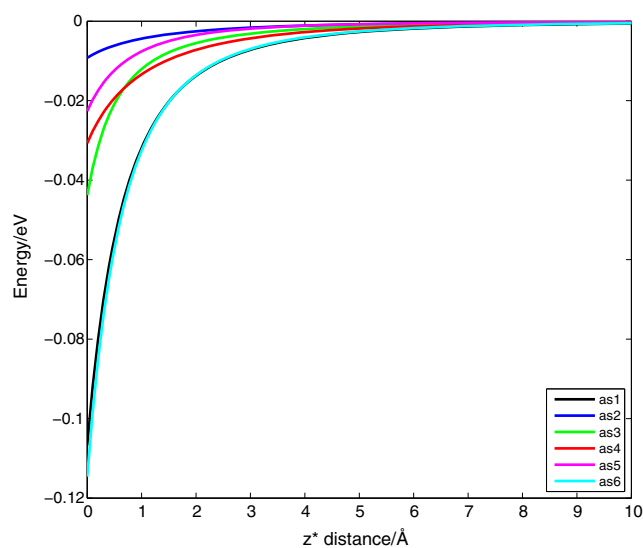


Fig. 9 Energy plots of the six orientations of the scorpion conformation of acetaminophen

in the conformation where the hydrogen is near the surface, though, **ac6** have gained 0.005 eV compared to **af6**, while **ac5** loses around 0.01 eV.

The vertical orientations, 3 and 4, have approximately the same interaction energy in the **ac** and **af** conformation. In the upright position, only the atoms near the surface contribute significantly to the energy. Since the difference between the two conformations are a 180° rotation of the hydroxy group, the energy is not affected in these orientations. When only the benzene ring and amide group or hydroxy group is considered, the two flat conformations are identical.

The scorpion conformation The scorpion conformation of acetaminophen has been investigated in six orientations as

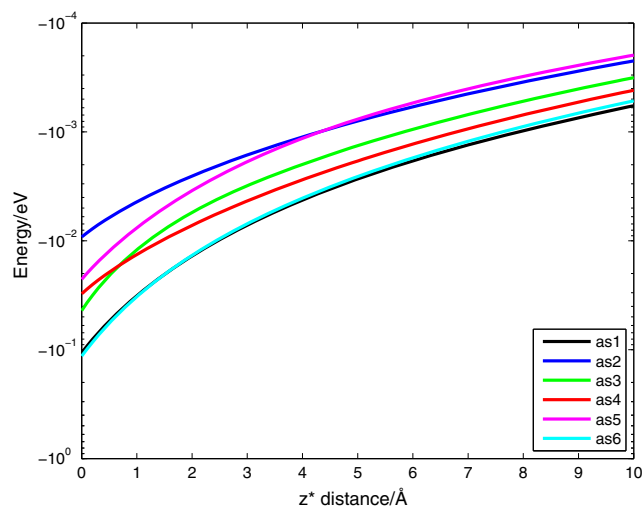
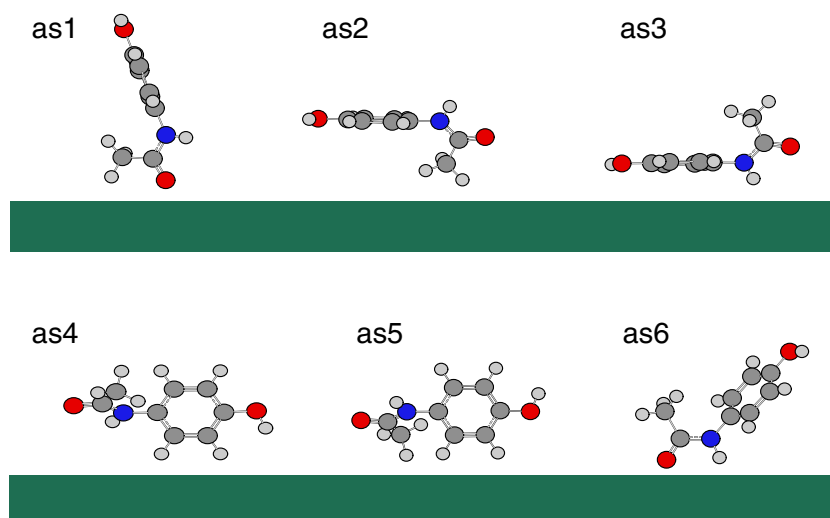
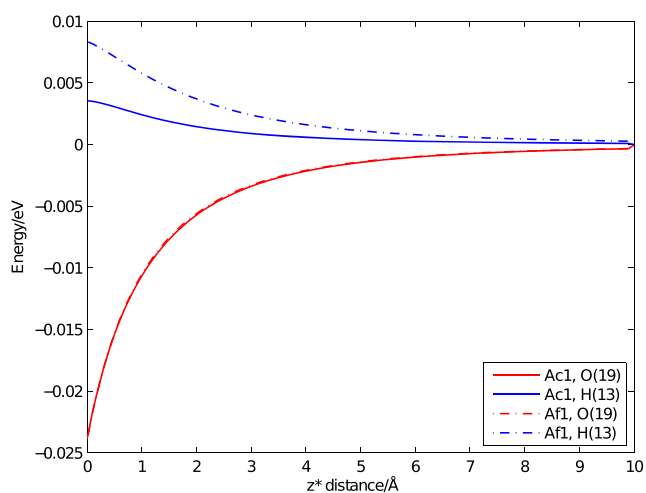


Fig. 10 Energy plots of the six orientations of the scorpion conformation of acetaminophen in a logarithmic scale

Fig. 11 The orientations of the scorpion conformation

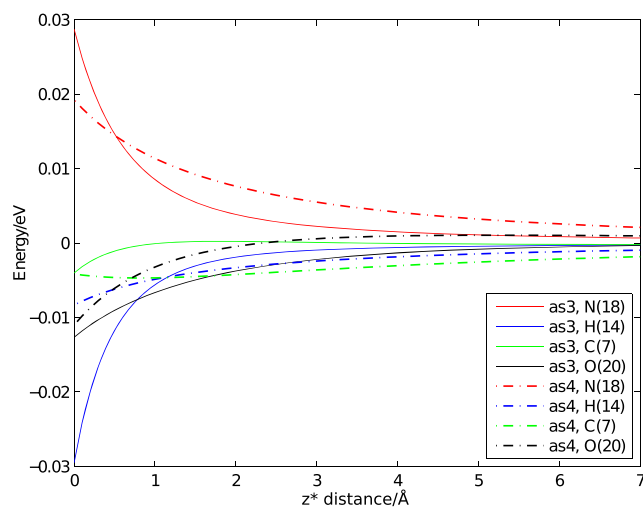
well, and the interaction energies can be seen in Figs. 9 and 10. The greatest interaction is observed for the orientations **as6** and **af1**, with **as6** having the lowest interaction energy. It is expected due to the negatively charged oxygen and nitrogen in the amide group, O(20) and N(18), that the two conformations have the lowest energies. Further, this explanation also justifies why the **as6** orientation has the lowest interaction energy (Figs. 11 and 12).

At $z^* = 0$, the **as3** orientation has the third lowest energy, which is due to the attraction between the amide nitrogen, N(18), and the hydroxy oxygen, O(19), and the corresponding induced charges. However, around $z^* = 1$ the **as4** orientation has lower interaction energy, and this is true for the longer distances as well. The orientation **as3** has lower interaction energy than **as4** at short distances because of the short distance between the charged atoms, H(14), N(18), O(19), and O(20), to the surface.

**Fig. 12** The energy contribution from the hydroxy group for ac1 and af1

In Figs. 13 and 14, the atomic contributions related to the overall interaction energy of the atoms in the amide and the hydrogen atoms in the benzene moiety are presented. For the **as3** orientation, the energy contribution related to N(18) is increased and the energy related to H(14) is decreased as the molecule approaches the surface, which implies a great negative charge being induced by the hydrogen. This effect is rather short ranged, and around 1 Å the effect is hardly seen. A similar but longer-ranged behavior is observed for the energy contributions related to N(18) in the **as4** orientation. The difference is that the repulsion arises from the negative charges mainly induced by H(14) and C(7), and at longer distances smeared out charges are better than localized.

The effect of the delocalized induced negative charges is evident internally in the molecule as well; the atoms further away from the amide group have lower energy in the **as4**

**Fig. 13** The atomic contribution to the overall interaction energy of the amide group

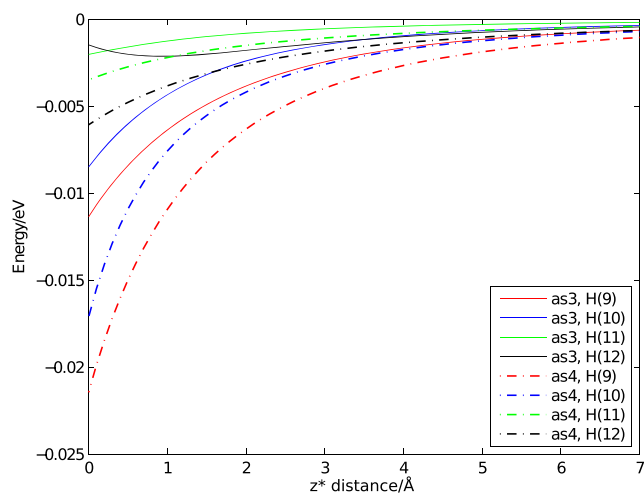


Fig. 14 The atomic contribution to the overall interaction energy of the benzene hydrogen atoms

orientation than in the **as3** orientation. In both orientations, the neighboring hydrogen atoms in the benzene moiety, H(10) and H(11), experience an attraction from the induced charges, but this time the energy contributions are lowest for the **as4** orientation. At first, it may come as a surprise that H(11), which is pointing away from the surface in **as4**, has a lower energy in **as4** than in **as3**, where it is closest to the surface. The reason is the same as before; the induced smeared out charges. H(9), in the other end of the benzene moiety, experiences an even greater attraction, which is due to the charges induced by H(13) in the hydroxy group. Since the oxygen is further away from the surface in the **as4** orientation than in **as3**, the corresponding induced charge is lower, and the effect on the atoms is lowered as well. The energy of the last hydrogen, H(12), in the benzene moiety in the **as4** orientation decreases as the molecule gets closer to the surface. At longer distances the same is true for H(12) in **as3**, but when the distance is shorter than 1 Å, the energy increases. This is due to the effect of the charge induced by O(19). Along with the smeared out positive charges H(9) and H(10) is closer to the surface in the **as4** orientation and thereby induces greater charge and can feel the other induced charges better. At longer distances, it is mainly the hydrogen atoms in the benzene moiety, which are responsible for **as4** having lower energy than **as3** (Table 2).

Table 2 The energy contributions from the different parts of the molecule having the scorpion conformation with the **as3**, **as4**, and **as5** orientations

| | $z^* = 0$ | Hydroxy | Benzene hydrogens | Benzene carbons | Acetamide |
|--------|-----------|---------|-------------------|-----------------|-----------|
| As3/eV | | -0.0090 | -0.0233 | 0.0056 | -0.0170 |
| As4/eV | | 0.0058 | -0.0569 | 0.0185 | 0.002 |
| As5/eV | | 0.0066 | -0.0286 | 0.0100 | -0.011 |
| | $z^* = 2$ | | | | |
| As3/eV | | 0.0023 | -0.0088 | 0.0025 | -0.0015 |
| As4/eV | | 0.00 | -0.0177 | 0.0052 | 0.0017 |

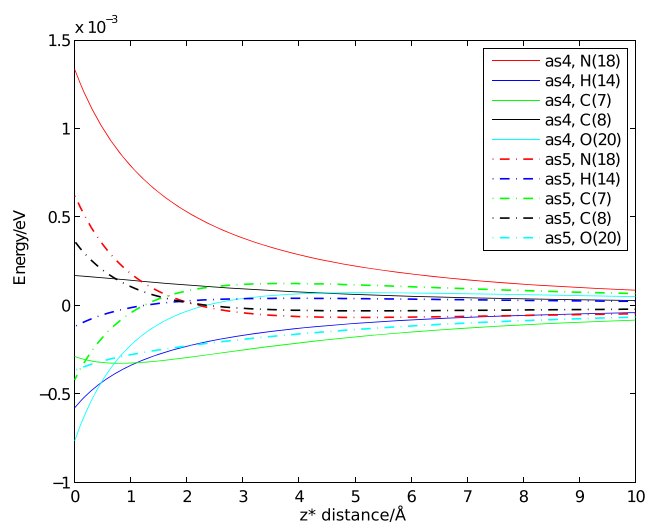


Fig. 15 Acetamide group

The lowest interactions at $z^* = 0$ are observed for the **as2** and **as5** orientations. The first has the disadvantage of the methyl group blocking the amide and hydroxy group approaching the surface. As a result, the interaction is remarkably lower than that observed for the rest of the orientations. The behavior of the **as5** orientation is somewhat more difficult to explain; one might expect a molecule in this orientation to behave similar to a molecule in the **as4** orientation. This is clearly not the case; for one thing there is a substantial energy difference at $z^* = 0$ (Table 2), and though decreasing, this difference seems to exist at longer distances as well. The nitrogen and oxygen atoms in the amide group are flipped up in the **as5** orientation compared to the **as4** orientation, and the increased distance accounts for some of the energy difference. This flip also shortens the distance of the amide hydrogen, H(14), and the surface, which induces a negative charge in the dielectric continuum. In Figs. 15, 16 and 17, the atomic contributions to the overall interaction energy of the acetamide and hydroxy subgroup, and of the hydrogens on the benzene moiety, are shown for the **as4** and **as5** orientation. Though having the lowest interaction energy, the **as4** orientation has the highest positive energy contribution from a single atom; the nitrogen in the amide

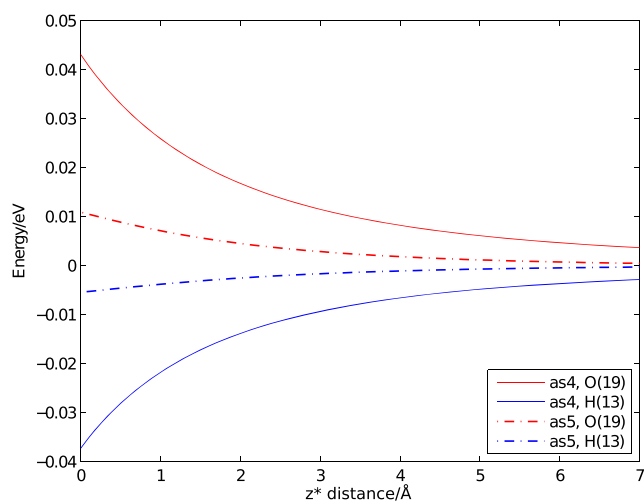


Fig. 16 Hydroxy group

group, N(18). The high energy contribution related to the nitrogen atom and the low energy contributions related to the H(14) and C(7) atoms suggest a strong induced negative charge in the dielectric medium. In the other end of the molecule, a similar event is observed; because a significant negative charge is induced by H(13), the energy of the H(13) is lowered and the energy O(19) is raised compared to the **as5** orientation. Further, the induced positive image charges by H(13) and H(14) lowers the energy of H(10) and H(9) more in **as4** than in **as5** (see Fig. 17). For all the conformations, the major difference in energy arises from the amide, where **as5** have the lowest energy due to H(14) being flipped up, and the hydrogens of the benzene moiety, where **as4** has the lowest energy due to the H(14) and H(13) being near the surface (Table 2). The impact of hydrogen on the interaction energy is surprising because of the low

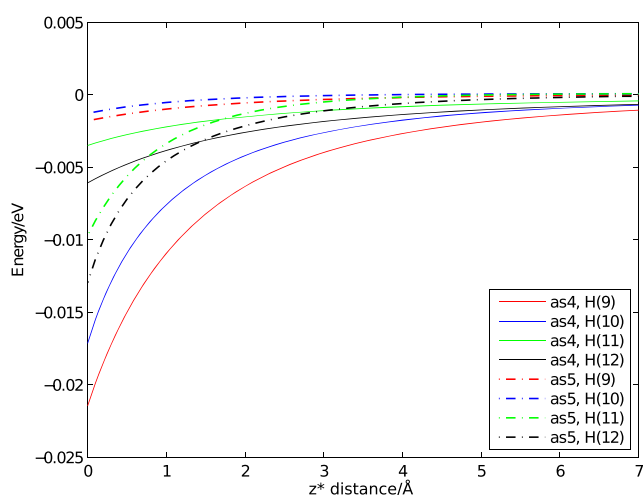


Fig. 17 Benzene hydrogen atoms

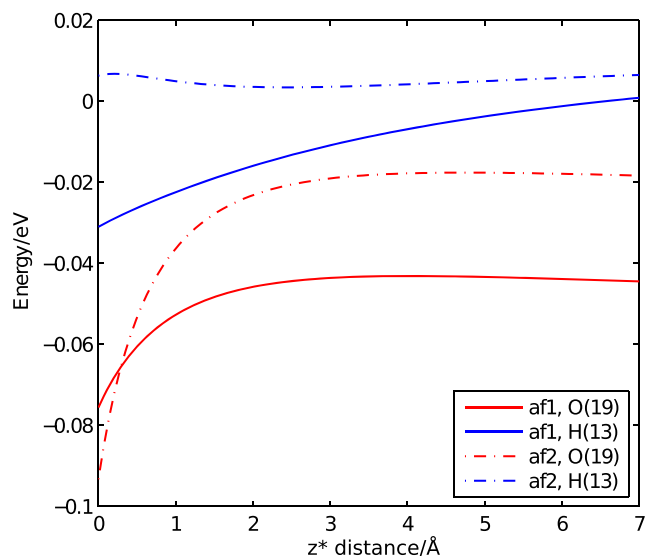


Fig. 18 Solvated **af1** and **af2** hydroxy group

partial charges, but nevertheless it is this interaction which gives the **as4** orientation its stability.

Comparison of the molecular conformation In line with the previous discussion of the orientations, the lowest interaction energy is achieved with the scorpion conformation and the **as6** orientation, because this geometry allows the nitrogen and oxygen atoms to be close to the surface, and the positive amide carbon to be furthest away. This results in the most stable interaction of the scorpion conformation, the energy being a factor of two greater than that of the flat **af** conformation and 0.04 eV greater than the flat **ac** conformation.

Though the scorpion conformation can obtain the lowest interaction energy, the energy of the molecule is 0.11 eV

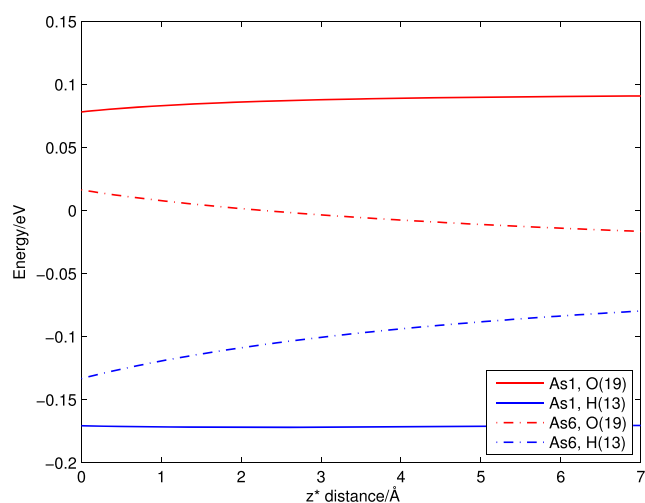


Fig. 19 Solvated **as1** and **as6** hydroxy group

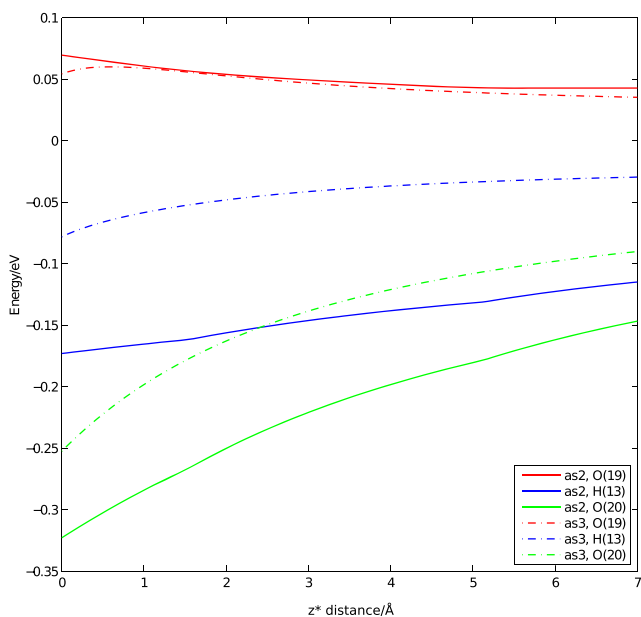


Fig. 20 Solvated **as2** and **as3** hydroxy group

higher than the energy of the flat conformation. Since the interaction energy difference of the most favorable orientation in the scorpion and the flat conformations is 0.04 eV, the conversion energy loss can be halved. This suggests that the molecular structure can be altered during aggregation on a polymer particle represented by a dielectric medium.

The two flat conformations have some differences as well. The major difference is the most stable orientation is changed from orientation 5 to 2 going from the **af** to the **ac** conformation.

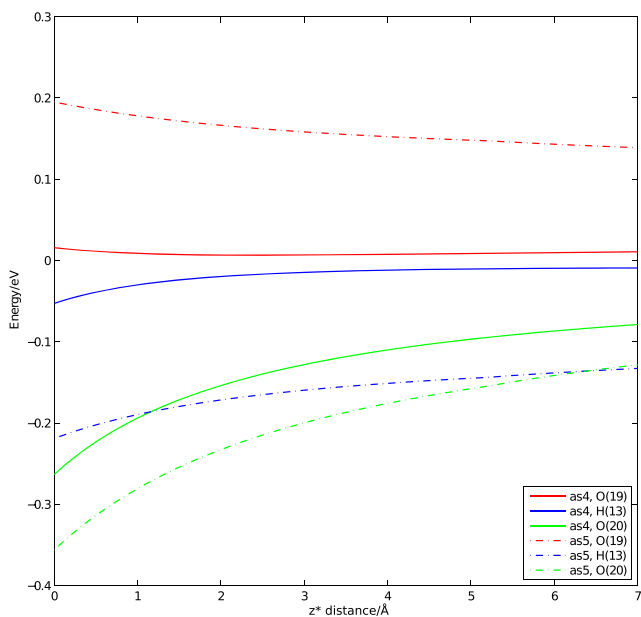


Fig. 21 Solvated **as4** and **as5** hydroxy group

The polymer and molecular system in solution

The flat **af conformation** The interaction energies of the different orientations and polymer particle along with the surrounding solvent are shown in Fig. 22. The relative stability at $z^* = 0$ is changed compared to that in vacuum, since the solvent interacts strongly with the molecular charge distribution. The larger dielectric constant of the solvent leads to larger induced image charges. A clear indication of this, is the **af6** orientation which was the second least stable orientation in vacuum, but the most stable when the solvent is taken into account. This is due to the amide oxygen, O(20), and the hydroxy group being so close to the solvent surface, and thus inducing larger image charges than in the solid. This is evident by comparison to the same orientation in vacuum, and the **af5** orientation, which is the **af6** orientation rotated 180°. The bump on the **af6** curve is caused by a shift in the atom determining the radius, at $z^* < 1.7$ H(12) is determining, while at $z^* > 1.7$ H(7) determines.

Though the opposite oriented conformation compared to **af6**, the **af5** orientation has the second lowest energy near the solid surface. The orientations **af5** and **af6** have the advantage over the other orientations of having the highly charged atoms pointing either towards the solvent surface or the polymer particle surface. When the distance to the particle is increased, the **af6** orientation remains the most stable orientation, while **af5** is overtaken by **af1** and **af4** before $z^* = 1.2$. When the distance to the surface is increased, the radius of the cavity is increased as well, resulting in the amide and hydroxy group being further way from the solvent. At longer distances, the larger charged oxygen atom's contribution is limited by the increased radius, which raises the energy. All the orientations, except **af3**, have the amide oxygen, the hydroxy group, or both

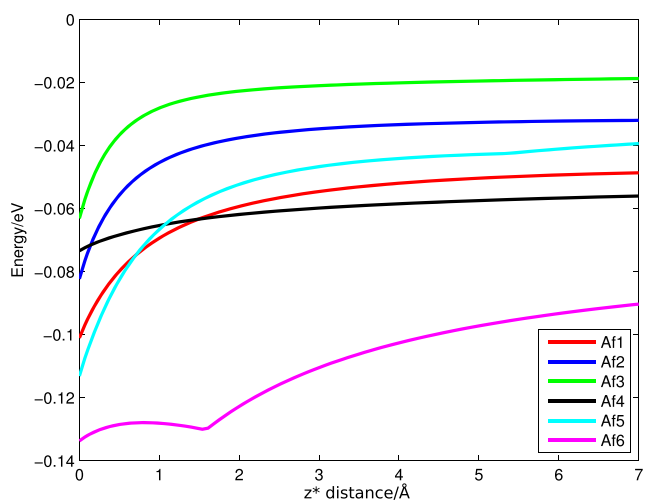


Fig. 22 Solvated **af** orientations

near the solvent surface, which accounts for the increased stability at longer distances.

The orientations parallel to the solid surface, **af1** and **af2**, are the third and fourth stable orientations near the surface of the polymer particle. They both have similar behavior when the distance is increased, which is expected due to the similarity in orientation. The difference in energy may, to some extent, be assigned to the difference in the cavity radius. Further, and more importantly, the hydroxy hydrogen, H(13), in **af2** does not gain any energy, opposite to the one in **af1** (Fig. 18). The reason may be that this hydrogen experiences the positive image charge induced by O(19) in the solvent, while the hydrogen itself is not inducing a large image charge, due to the increased distance to the surface. The enhanced atom–solvent distance for hydrogen compared to oxygen is due to the slightly tilted molecule.

The last two orientations, **af3** and **af4**, are the least stable near the surface of the polymer particle. As before, the relative stability of the two are reversed as compared to that in vacuum. The least stable orientation, **af3**, gains very little compared to the other orientations due to the fact that the methyl group is insulating the whole molecule from the solvent by the larger radius. The orientation **af4**, on the other hand, gains a lot by interacting with the solvent, but very little from the interacting with the polymer particle. This is evident since the energy is lowered by only 0.01 eV when the molecule goes from $z^* = 7 \text{ \AA}$ to 0 \AA . At all distances, the radius of the cavity is determined by hydroxy group, ensuring a constant energy reduction (Figs. 19, 20, 21, 22, 23 and 24).

The ac conformation The same relative stability of the orientations of the solvated flat conformations is the same, but the **ac** conformation generally obtains lower energies, Fig. 24.

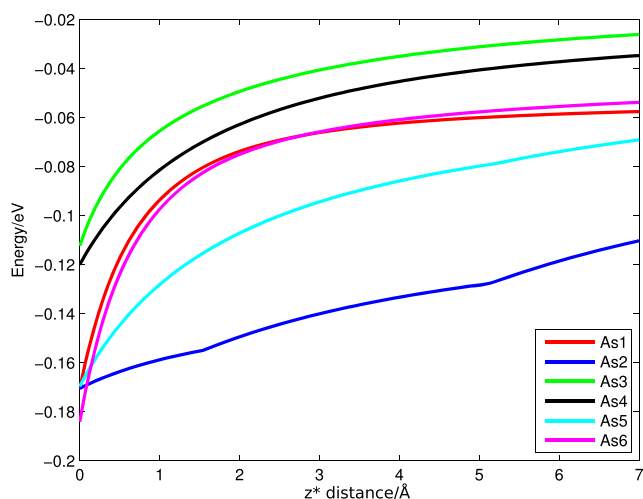


Fig. 23 Solvated as orientations

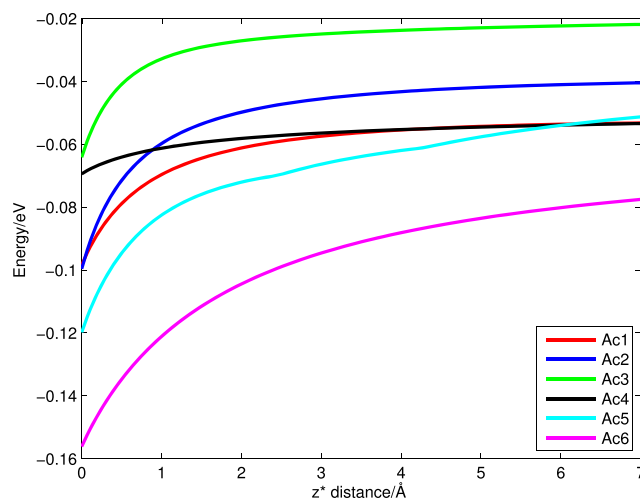


Fig. 24 Solvated Ac

As in vacuum the vertical orientations, 3 and 4, have approximately the same energy in both flat conformations. The same is true for orientation 2, while orientation 1 is lowered 0.02 eV going from the **af** to the **ac** conformation. The main reason is H(13), which goes from contributing with a slightly positive energy in the **af** conformation, to contributing negative (-0.027 eV) in **ac**. The two hydrogen atoms on the H(14) side, H(11) and H(12), are lowered in energy, while for the hydrogen atoms on the opposite side it is raised, Fig. 25. This matches the idea that H(13) in **ac** is close to positive or neutral charges, which are near the surface. Thus H(13) is close to more induced negative charges in **ac** than in **af**.

It is worth noting that orientation 6 gains around -0.02 eV going from the **af** conformation to **ac**, while orientation 5 only gains -0.01 eV . This is due to a lower energy contribution from the hydroxy group and O(20). In **ac5**

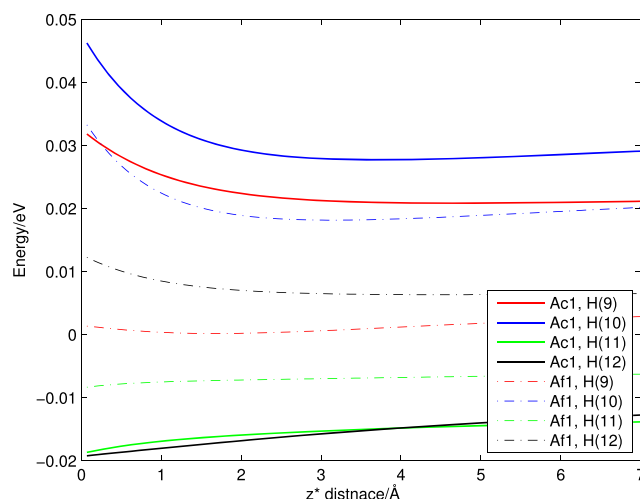


Fig. 25 Energy contribution from the benzene hydrogen in ac1 and af1

H(13) and H(14) are close to the solvent surface and, thus, they contribute greatly to the energy. The two oxygen atoms do not induce strong charges, but are affected by the charges produced by H(13) and H(14). In **ac6** this is reversed and the oxygen atoms are closest to the solvent surface. Due to the greater charge of the oxygen, greater charges are induced in the solvent-medium. The significant difference between **ac5** and **6** is O(20), C(7), and H(14), which accounts for the increased stability of orientation **6**, Fig. 26.

The scorpion conformation The interaction energies of the different orientations of the scorpion conformation and polymer particle surrounded by solvent are shown in Fig. 23. In vacuum, when solvated, we expect the opposite to be the case: The amide or hydroxy group is, in the most stable orientations, expected to be near the solvent surface.

When that is said, at the surface of the polymer particle the most stable form is, as in vacuum, the **as6** orientation closely followed by the orientations **af1**, **as2**, and **as5**. Overall the orientations **af1** and **as6** behave similarly as in vacuum, but the energies are lowered due to the interactions with the surrounding solvent. The orientation **as6** is lowered somewhat more because of the hydroxy oxygen, O(19), having a lower energy due to the image charge induced by the hydrogen H(13), see Fig. 23. In the **af1** orientation the image charge induced by H(13) is close to the atom O(19), while it is further away in the **as6** orientation, due to the angle between the position vectors of O(19) and H(13) being larger in the **as6** orientation.

The two conformations with energies almost the same as the **af1** orientation at $z^* = 0$, **as2** and **as5**, have lowered the energy the most. When the distance is increased to around 0.2 Å both orientations have lower energy than the rest of the orientations. The **as2** orientation has two bumps due to

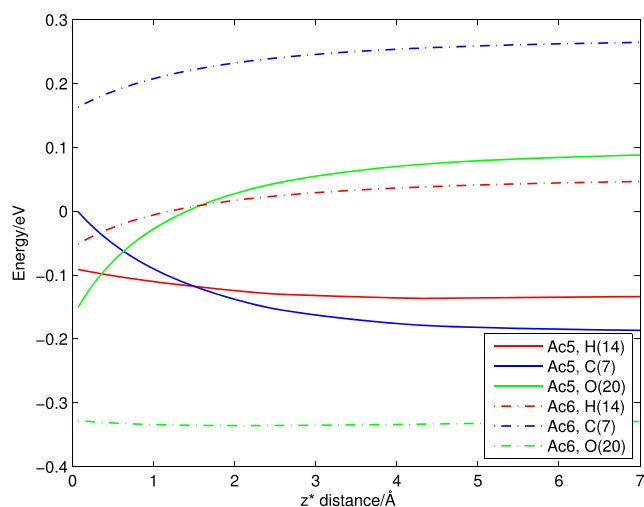


Fig. 26 Energy contribution from O(20), C(7), and H(14) in the amide group in **ac5** and **ac6**

a change in which atom determines the radius of the cavity. The radius is determined by H(13) between $z^* = 0$ Å to 1.61 Å, by O(19) between 1.61 Å and 5.32 Å, and by H(14) at longer distances than 5.32 Å.

The **as2** orientation has the lowest energy at $z^* > 0.2$ because both oxygen atoms are close to the solvent surface. The **as3** orientation, which is the **as2** orientation rotated 180°, decreases little in energy compared to **as2**, because the radius of the half-sphere is determined by the methyl group. The hydroxy group is therefore further away from the solvent surface, and, consequently, the stabilizing contribution from this group is lower, see Fig. 20.

As observed previously, the relative stability of two related orientations is reversed when going from vacuum to solvation, and this hold for the **as4** and **as5** orientations as well. A part of the extra stability of the **as5** orientation comes from the amide oxygen being slightly closer to the surface of the solvent than in the **as4** orientation, see Fig. 21. The other contribution comes from the hydroxy hydrogen inducing a charge in the vicinity of atoms H(9) and H(10).

Comparison of the flat conformations and scorpion conformation As in vacuum, the energy of the scorpion conformation is lower than the flat conformations when they are solvated. The flat conformations are reduced a bit more than the scorpion conformation, but the energy difference between the most stable orientations of the flat **ac** and scorpion conformation is still around 0.02 eV.

The interactions between the atom O(20) and the polymer surface is the strongest, and when combined with N(18), the lowest interaction energies are obtained. If they are blocked from getting close to the surface by the rest of the molecule, the surrounding positive lower-charged atoms have a significant role to play. Since the positive charge is distributed between more atoms than the negative charge, the charges are generally lower and the charge distribution more diffuse. The delocalized charges can in some cases interact over longer distances than the atoms O(20) and N(18), and stabilizing an orientation through the, at first sight innocent, hydrogen atoms in the benzene moiety.

Investigating the role of polymer and solvent dielectric constants Within the presented heterogenous dielectric solvation model, it is straightforward to investigate the role of different solvents and polymers. Polymers have dielectric constants from 1 to 20, while solvents can have dielectric constants from about 2 (cyclohexane) to above 100 (formamide). In Fig. 3 we compare the influence of these extreme situations on the aggregation of the flat (**ac**) conformation of acetamide.

The two known crystal forms of acetaminophen have significantly different intermolecular packing patterns. The sideways stacking of molecules on the polymer surface

(orientations **5** and **6**) were the most stable. In both crystal forms, a slab of molecules can be identified showing the sideways stacking pattern, however in the orthorhombic form, this slab consists of only orientation **5**, whereas in the case of the monoclinic form, both orientation **5** and the reverse orientation **6** are involved (Fig. 2).

To suppress the formation of the monoclinic polymorph and favor the formation of the orthorhombic form, it is necessary to choose a solvent with a high dielectric constant combined with a surface with a low dielectric constant, e.g., combining water with poly tetrafluoroethylene (TEFLON). As shown in Fig. 3b, the energy gap between the two sideways conformations **as5** and **as6** is more than 0.05 eV per molecule (about 130 kJ/mol). If instead the monoclinic form is preferred, a combination involving heptane and a high-dielectric solid such as graphite should be used; this will favor both conformations **5** and **6**, and thus allow the monoclinic polymorph to nucleate on the surface.

Conclusions

We have investigated the prospects of using a heterogeneous dielectric solvation model to study the nucleation of molecular crystals on polymer surfaces. We demonstrate that the orientation of the molecule has a major influence on the interaction energy, and hence the likelihood of the molecule aggregating on the surface. In the case of acetaminophen, the least stable gas-phase conformation (scorpion) is the form having the most favorable interaction with the surface. This conformation is not observed in the known crystal forms, but our model suggests that heterogeneous nucleation on a polymer surface can be used to initiate aggregation of such otherwise metastable crystal nuclei by tuning the dielectric constants of solvent and polymer.

It is important to note that the inclusion of the outer solvation changes the relative stability of the orientations and between the two conformations. Neglecting a solvent with a significantly higher dielectric constant will in many cases result in wrong results and predictions. This is pronounced in the flat conformations where the relative stabilities of the orientations 1–2, 3–4, and 5–6 (Fig. 6) are reversed when going from vacuum to solvation.

The model suggests that the aggregation on a polymer surface will allow the nucleation of the orthorhombic form of acetaminophen, in line with experimental evidence. The preference for the nucleation of the orthorhombic polymorph is pronounced when an apolar surface is combined with a polar solvent.

By using the heterogeneous dielectric solvation model described here, it is straightforward to change dielectric constants, and hence to study the effect of other solvents and other surfaces. This may inspire the experimentalist

in the choice of solvent and polymer for crystallization of polymorphic systems.

Our approach demonstrates a non-epitaxial approach to heterogeneous nucleation. It is a computationally inexpensive approach which, once the atomic charges have been derived from ab initio calculations, scales linearly with the size of the molecules, and it is thus possible to study the aggregation of very large molecules.

In our present investigation, we have not included any explicit solvent molecules in the description of the solvent interactions between the heterogeneously solvated molecule and the neighboring solvent molecules. It is clearly, as indicated by one of the reviewer, a very important aspect to consider in future investigations utilizing the presented method. In the present investigation, we have not included van der Waals interactions between the molecule and the polymer but we have in ref. [71] developed a model that includes dispersion interactions between the polymer and the molecule. We have clearly shown that dispersion interactions are important for describing the interactions between the polymer and the molecule [71]. For future investigations, it would be beneficial to combine the two approaches when investigating the interactions between the polymer and molecule. Presently, we are trying to establish procedures for checking how well the model is able to explain and predict experimental results but we are still in the initial phase of utilizing the presented model.

References

- Gavezzotti A (1995) *J Am Chem Soc* 117:12299–12305
- Gavezzotti A (2002) *Cryst Eng Comm* 4(61):343–347
- Haleblan J, McCrone W (1969) *J Pharm Sci* 58:911–929
- Morisette SL, Soukasene S, Levinson D, Cima MJ, Almarsson O (2003) *Proc Nat Acad Sci* 100:2180–2184
- Bernstein J (2008) *Polymorphism in molecular crystals*
- Day GM, Cooper TG, Cruz-Cabeza AJ, Hejczyk KE, Ammon HL, Boerrigter SXM, Tan JS et al (2009) *Acta Cryst B* 65:107–125
- Kendrick J, Leusen FJJ, Neumann MA, van de Streek J (2011) *Prog Cryst Struc Pred Chem* 17:10736–10744
- Madsen AØ, Larsen S (2007) *Ang Chemie Int Ed* 46:8609–8613
- Madsen AØ, Mattson R, Larsen S (2011) *J Phys Chem A* 115:7794–7804
- Jarzemska KN, Hoser AA, Kaminski R, Madsen AØ, Durka K, Wozniak K (2014) *Cryst Growth Des* 17:3453–3465
- Nyman J, Day GM (2015) *Cryst Eng Comm* 17:5154–5165
- Wahlberg N, Ciochon P, Petricek V, Madsen AØ (2014) *Cryst Growth Des* 14:381–388
- Weissbuch I, Lahav M, Leiserowitz L (2003) *Crys Growth Des* 3:125–150
- Weissbuch I, Shimon LJW, Landau EM, Popovitzbiro R, Berkovitchyellin Z, Addadi L, Lahav M, Leiserowitz L (1986) *Pure Appl Chem* 58:947–954
- Weissbuch I, Zbaida D, Addadi L, Leiserowitz L, Lahav MJ (1987) *J Am Chem Soc* 109:1869–1871
- Weissbuch I, Addadi L, Lahav M, Leiserowitz L (1991) *Science* 253:637–645

17. Price CP, Grzesiak AL, Matzger AJ (2005) *J Am Chem Soc* 127:5512–5517
18. Ockwig N, Yaghi O, Matzger AJ (2006) *Ang Chemie Int Ed*
19. Foroughi LM, Kang Y-N, Matzger AJ (2011) *Cryst Growth Des* 11:1294–1298
20. Boldyreva EV, Drebuschak VA, Paukov IE, Kovalevskaya YA, Drebuschak TN (2004) *J Therm Anal Cal* 77:607–623
21. Lopez-Mejias V, Knight JL, Brooks CL, Matzger JA (2011) *J Langmuir* 27:7575–7579
22. Newton MD (1975) *J Phys Chem* 79:2795
23. Noell JO, Morokuma K (1975) *Chem Phys Lett* 36:465
24. Beveridge DL, Schnuelle GW (1975) *J Phys Chem* 79:2562
25. Hylton J, Christoffersen RE, Hall GG (1974) *Chem Phys Lett* 24:501
26. Contreras R, Aizman A (1985) *Int J Quant Chem* 27:193
27. Hoshi H, Sakurai M, Inone Y, Chujo R (1987) *J Chem Phys* 87:1107
28. Tapia O (1980) Molecular interactions. In: Ratajczak H, Orville-Thomas WJ (eds). Wiley, New York
29. Warshel A (1978) *Chem Phys Lett* 55:454
30. Sanchez-Marcos E, Terryn B, Rivail JL (1985) *J Phys Chem* 87:4695
31. Rinaldi D (1982) *Comput Chem* 6:155
32. Tapia O (1980) Quantum theory of chemical reactions. In: Daudel R, Pullman A, Salem L, Veillard A (eds), vol 3. Wiley, Dordrecht, p 25
33. Karlström G (1989) *J Phys Chem* 93:4952
34. Karelson M, Zerner M (1990) *J Am Chem Soc* 112:9405
35. Day PN, Jensen JH, Gordon MS, Webb SP, Stevens WJ, Krauss M, Garmer D, Basch H, Cohen D (1996) *J Chem Phys* 105:1968
36. Chen W, Gordon MS (1996) *J Chem Phys* 105:11081
37. Cramer CJ, Truhlar DG (1991) *J Am Chem Soc* 113:8305
38. Cramer CJ, Truhlar DG (1992) *Science* 256:213
39. Mikkelsen KV, Dalgaard E, Svanstøm P (1987) *J Phys Chem* 91:3081
40. Mikkelsen KV, Ågren H, Aa Jensen HJ, Helgaker T (1988) *J Chem Phys* 89:3086
41. Mikkelsen KV, Jørgensen P, Aa Jensen HJ (1994) *J Chem Phys* 100:6597–6607
42. Mikkelsen KV, Luo Y, Ågren H, Jørgensen P (1994) *J Chem Phys* 100:8240
43. Mikkelsen KV, Luo Y, Ågren H, Jørgensen P (1995) *J Chem Phys* 102:9362
44. Mikkelsen KV, Sylvester-Hvid KO (1996) *J Phys Chem* 100:9116
45. Di Bella S, Marks TJ, Ratner MA (1994) *J Am Chem Soc* 116:4440
46. Yu J, Zerner MC (1994) *J Chem Phys* 100:7487
47. Cammi R, Cossi M, Mennucci B, Tomasi J (1996) *J Chem Phys* 105:10556
48. Willetts A, Rice JE (1993) *J Chem Phys* 99:426
49. Cammi R, Cossi M, Tomasi J (1996) *J Chem Phys* 104:4611
50. Wong MW, Frisch MJ, Wiberg KB (1991) *J Am Chem Soc* 113:4776
51. Angyan JG (1995) *Chem Phys Lett* 241:51
52. Olivares del Valle FJ, Tomasi J (1991) *Chem Phys* 150:139
53. Chipot C, Rinaldi D, Rivail JL (1991) *Chem Phys Lett* 191:287
54. Cramer CJ, Truhlar DG (1999) *Chem Rev* 99:2161
55. Tomasi J, Cammi R, Mennucci B (1999) *Int J Quant Chem* 75:783
56. Christiansen O, Mikkelsen KV (1999) *J Chem Phys* 110:1365
57. Poulsen TD, Kongsted J, Osted A, Ogilby PR, Mikkelsen KV (2001) *J Chem Phys* 115:2393–2400
58. Poulsen TD, Ogilby PR, Mikkelsen KV (2001) *J Chem Phys* 115:7843–7851
59. Poulsen TD, Ogilby PR, Mikkelsen KV (2002) *J Chem Phys* 116:3730–3738
60. Nymand TM, Åstrand P-O, Mikkelsen KV (1997) *J Phys Chem B* 101:4105
61. Jensen L, Schmidt OH, Mikkelsen KV, Åstrand P-O (2000) *J Phys Chem B* 104:10462
62. Osted A, Kongsted J, Mikkelsen KV, Christiansen O (2004) *J Phys Chem A* 108:8646–8658
63. Jørgensen S, Ratner MA, Mikkelsen KV (2001) *J Chem Phys* 115:3792
64. Jørgensen S, Ratner MA, Mikkelsen KV (2001) *J Chem Phys* 115:8185
65. Jørgensen S, Ratner MA, Mikkelsen KV (2002) *J Chem Phys* 116:10902
66. Frisch MJ, Trucks GW, Schlegel HB, Scuseria GE, Robb MA, Cheeseman JR, Montgomery JA Jr, Vreven T, Kudin KN, Burant JC, Millam JM, Iyengar SS, Tomasi J, Barone V, Mennucci B, Cossi M, Scalmani G, Rega N, Petersson GA, Nakatsuji H, Hada M, Ehara M, Toyota K, Fukuda R, Hasegawa J, Ishida M, Nakajima T, Honda Y, Kitao O, Nakai H, Klene M, Li X, Knox JE, Hratchian HP, Cross JB, Bakken V, Adamo C, Jaramillo J, Gomperts R, Stratmann RE, Yazyev O, Austin AJ, Cammi R, Pomelli C, Ochterski JW, Ayala PY, Morokuma K, Voth GA, Salvador P, Dannenberg JJ, Zakrzewski VG, Dapprich S, Daniels AD, Strain MC, Farkas O, Malick DK, Rabuck AD, Raghavachari K, Foresman JB, Ortiz JV, Cui Q, Baboul AG, Clifford S, Cioslowski J, Stefanov BB, Liu G, Liashenko A, Piskorz P, Komaromi I, Martin RL, Fox DJ, Keith T, Al-Laham MA, Peng CY, Nanayakkara A, Challacombe M, Gill PMW, Johnson B, Chen W, Wong MW, Gonzalez C, Pople JA (2004) Gaussian, Inc., Wallingford, CT
67. Cioslowski J (1989) *Phys Rev Lett* 62:1469
68. Cioslowski J (1989) *J Am Chem Soc* 111:8333
69. Åstrand P-O, Ruud K, Mikkelsen KV, Helgaker T (1998) *J Phys Chem A* 102:7686
70. Breneman CM, Wiberg KB (1990) *J Comp Chem* 11:361–73
71. Wahlberg N, Madsen AØ, Mikkelsen KV Accepted in *J. Mol. Mod.* <https://doi.org/10.1007/s00894-018-3664-1>